Electronic Supplementary Material (ESI) for Polymer Chemistry.

Ultrahigh volatile iodine capture by conjugated microporous polymer based on N,N,N',N'-tetraphenyl-1,4-phenylenediamine

Shun Wang, Yuchuan Liu, Yu Ye, Xianyu Meng, Jianfeng Du, Xiaowei Song and Zhiqiang Liang**

State Key Lab of Inorganic Synthesis and Preparative Chemistry, Jilin University,

Changchun, 130012, P. R. China.
E-mail: xiaoweisong@jlu.edu.cn; liangzq@jlu.edu.cn

Characterization

Powder X-ray diffraction (PXRD) patterns were collected on a Rigaku D-Max 2550 diffractometer using Cu-Kα radiation (λ = 0.15418 nm) in a 2θ range of 4-40° at room temperature. Fourier transform infrared (FT-IR) spectra were recorded in the range of 400-4000 cm^{-1} on a Nicolet 6700 FT-IR spectrometer with KBr pellets. Thermogravimetric analyses (TGA) were performed on a Perkin-Elmer TGA-7 thermogravimetric analyzer from room temperature to 800 ℃ in nitrogen atmosphere with a heating rate of 10 °C/min. Scanning electron microscopy (SEM) was performed on a JSM-6700F electron microscope. Fluorescence spectra were recorded on a FLUOROMAX-4 fluorescence spectrophotometer. Absorption spectra were recorded on a Hitachi U-4100 UV-vis spectrophotometer. The forms of iodine element loaded in CMPs were studied on an ESCALAB250 X-ray photoelectron spectroscopy. The solid-state ^{13}C cross-polarization/magic-angle spinning (CP/MAS) NMR spectra were collected a Bruker AVANCE III 400 WB spectrometer. ^{1}H NMR spectra were recorded at room temperature using a Varian Mercury spectrometer operating at frequencies of 300 MHz for ^{1}H. All gases adsorption-desorption measurements at different temperature were carried out on a Micromeritics ASAP 2020 instrument. The testing samples were degassed at 100 ℃ under vacuum for 12 h. The pore size distributions were derived from the adsorption branches using the nonlocal density functional theory (NLDFT) approach.

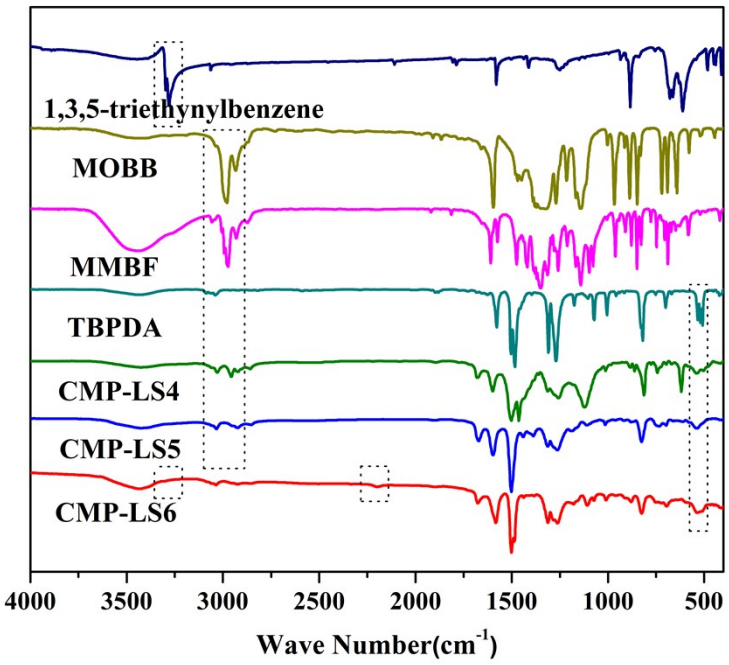

Fig. S1 IR spectra of monomers and polymers.

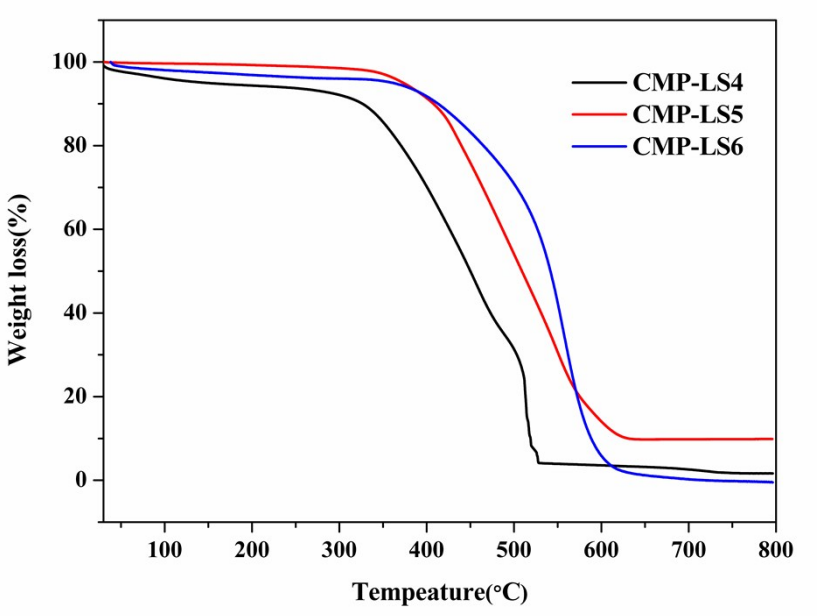

Fig. S2 TGA curves of **CMP-LS4–6** under air atmosphere.

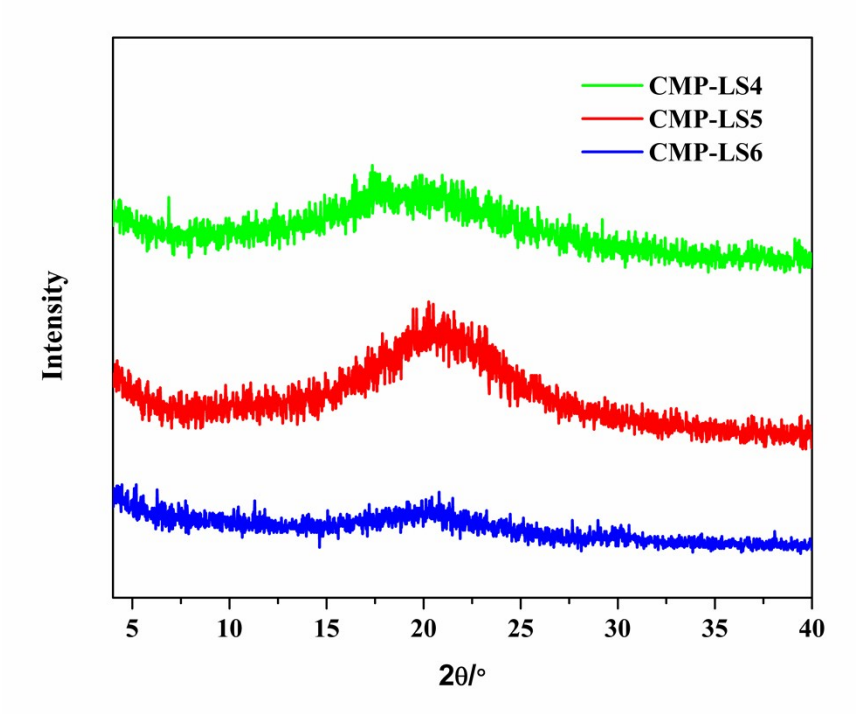

Fig. S3 Powder X-ray diffraction profiles of **CMP-LS4–6**.

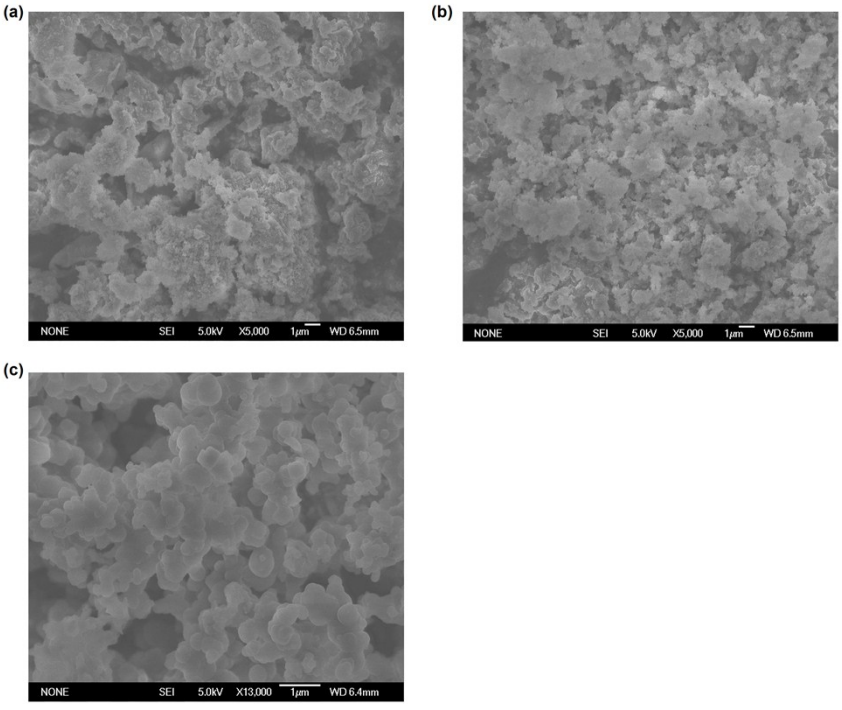

Fig. S4 FE-SEM images of (a) **CMP-LS4**, (b) **CMP-LS5** and (c) **CMP-LS6**.

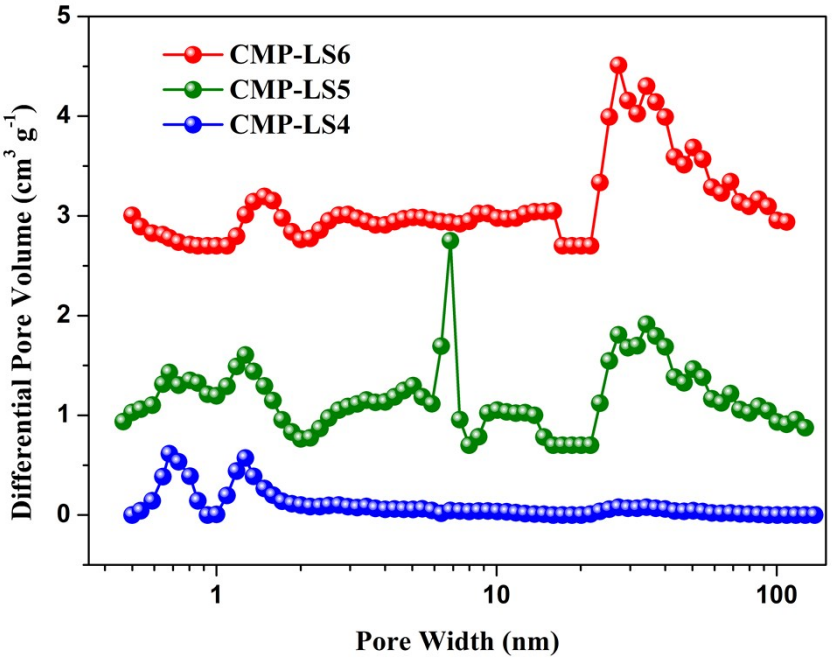

Fig. S5 Pore size distributions calculated using the non-local density functional theory (NLDFT) method.

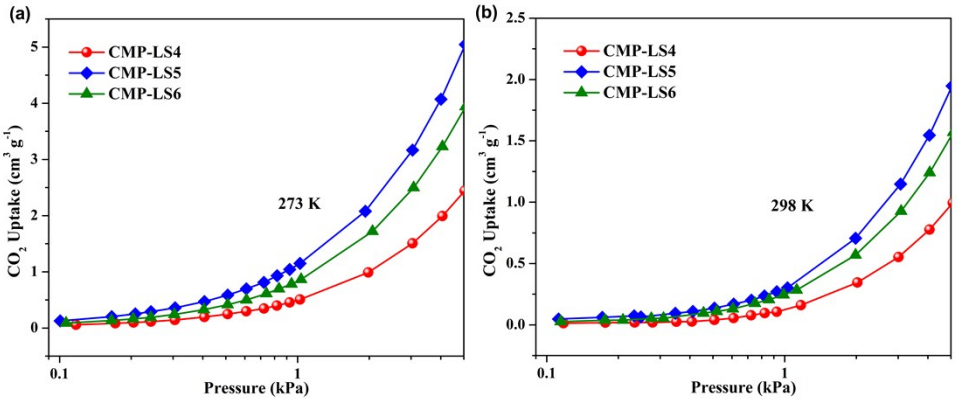

Fig. S6 CO_2 isotherms at the low-pressure region with log scale at 273/298 K.

Calculations of the Isosteric Heats of Gas Adsorption (Q_{st})

A virial-type expression comprising the temperature-independent parameters a_i and b_j was employed to calculate the enthalpies of adsorption for CO_2, the data were fitted using the equation:

$$lnP = lnN + {}^{1}/_{T} \sum_{i=0}^{m} a_i N^i + \sum_{j=0}^{n} b_j N^j$$

Here, P is the pressure expressed in Torr, N is the amount adsorbed in mmol g^{-1}, T is the temperature in K, a_i and b_j are virial coefficients, m, n represent the number of

coefficients required to adequately describe the isotherms (m and n were gradually increased until the contribution of extra added a and b coefficients was deemed to be statistically insignificant towards the overall fit, and the average value of the squared deviations from the experimental values was minimized). The values of the virial coefficients a_0 through am were then used to calculate the isosteric heat of adsorption using the following expression.

$$Q_{st} = -R\sum_{i=0}^{m} a_i N^i$$

Q_{st} is the coverage-dependent isosteric heat of adsorption and R is the universal gas constant. The heat of gas sorption for **CMP-LS4–6** in this manuscript are determined by using the sorption data measured in the pressure range from 0-1 bar (273 and 298 K for CO_2).

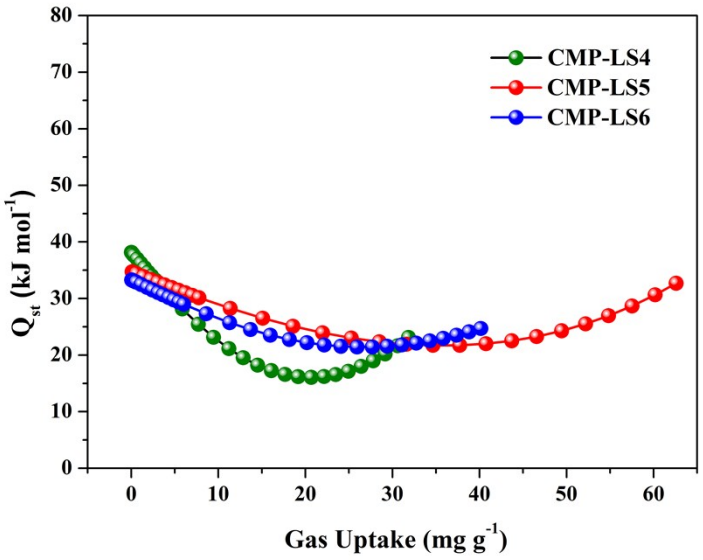

Fig. S7 Isosteric heats of adsorption of CO_2 for **CMP-LS4–6**.

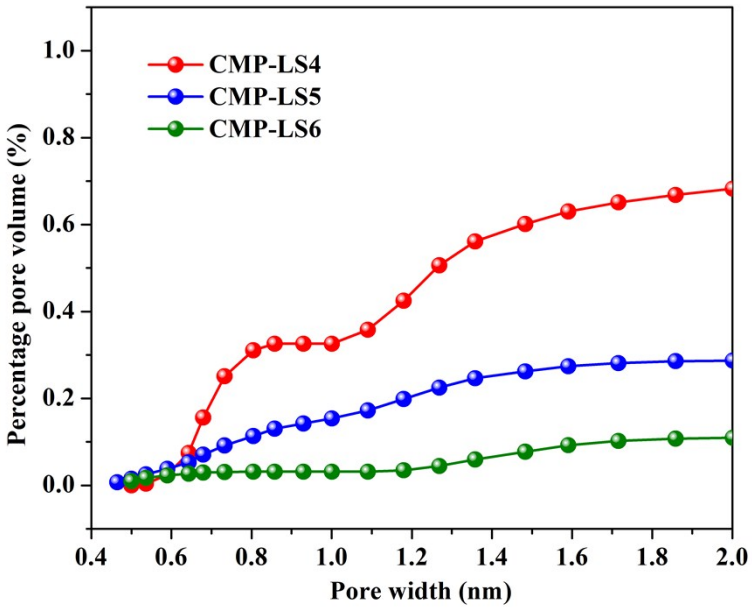

Fig. S8 Percentage pore volume isotherms of **CMP-LS4**–**6**.

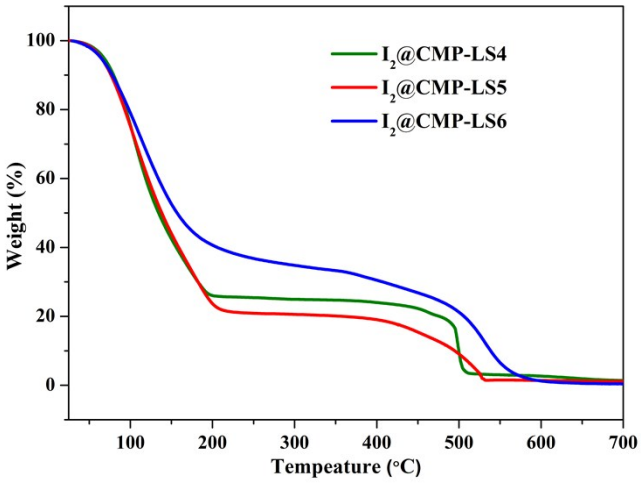

Fig. S9 TGA curves of **I_2@CMP-LS4–6**.

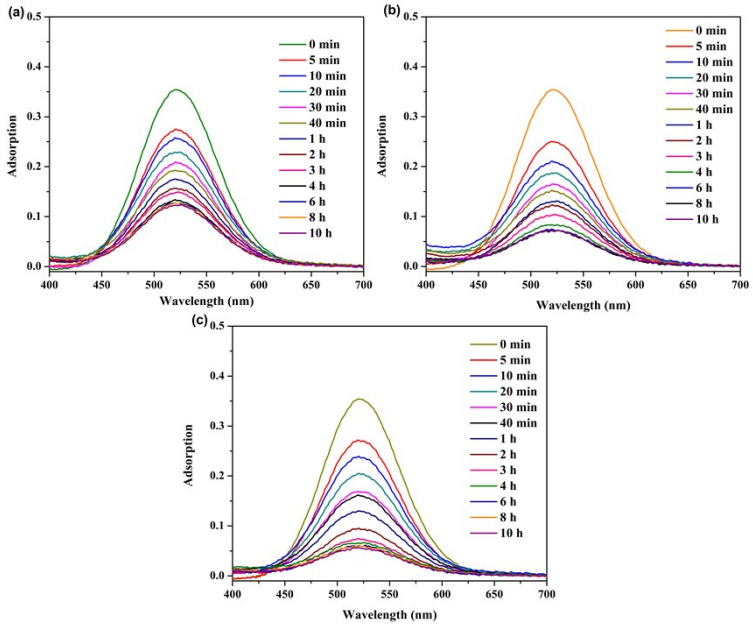

Fig. S10 UV-vis spectra at different times for **CMP-LS4** (a), **CMP-LS5** (b), and **CMP-LS6** (c) (10 mg) and iodine (200 mg L^{-1}, 5 ml) in hexane solution.

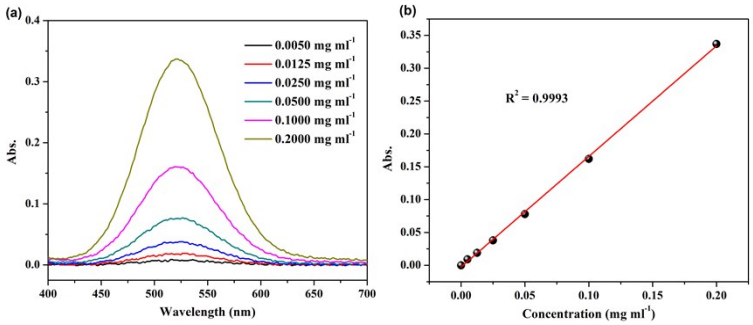

Fig. S11 (a) Calibration plots of standard iodine by UV/vis spectra in cyclohexane solution, (b) the fitting of Abs value vs concentration of I_2 with the relatively good linearity satisfies Lambert-Beer Law.

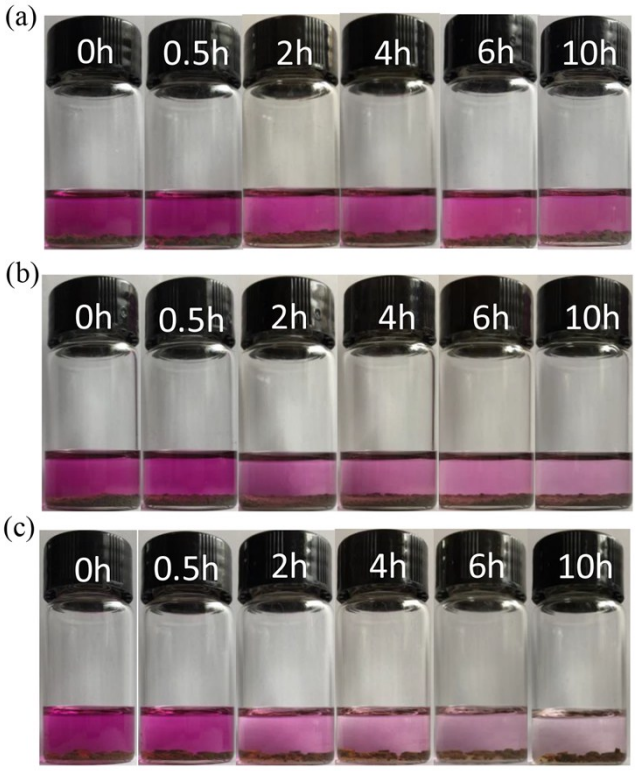

Fig. S12 Photographs demonstrating the iodine absorption capacity of (a) **CMP-LS4**, (b) **CMP-LS5**, and (c) **CMP-LS6** in hexane solution. The same weight of each CMPs (10 mg) were immersed in the iodine solution (200 mg mL^{-1}, 3 mL) at 25 ℃.

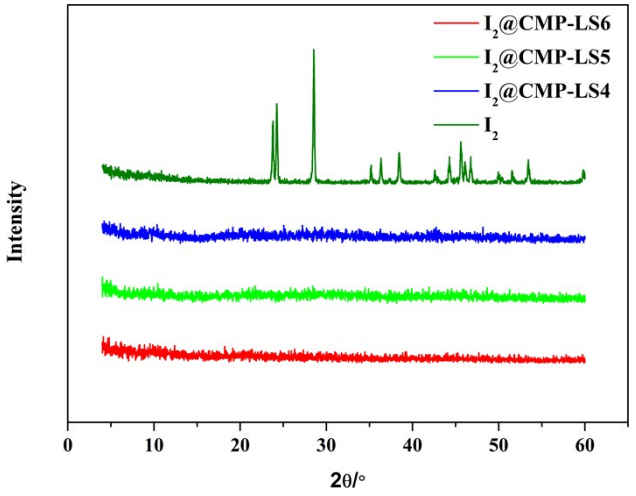

Fig. S13 XRD patterns of I_2, **I_2@CMP-LS4**, **I_2@CMP-LS5** and **I_2@CMP-LS6**.

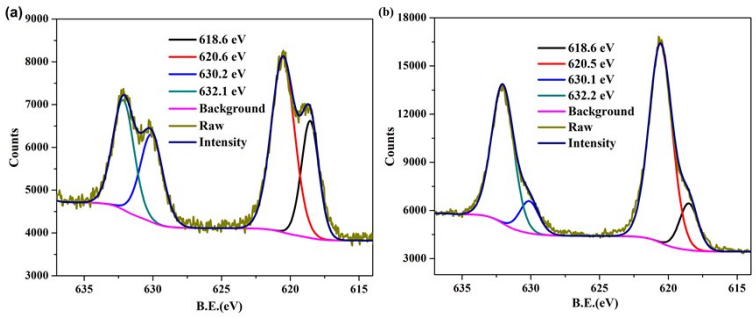

Fig. S14 XPS spectra of (a) **I_2@CMP-LS4**, and (b)**I_2@CMP-LS6**.

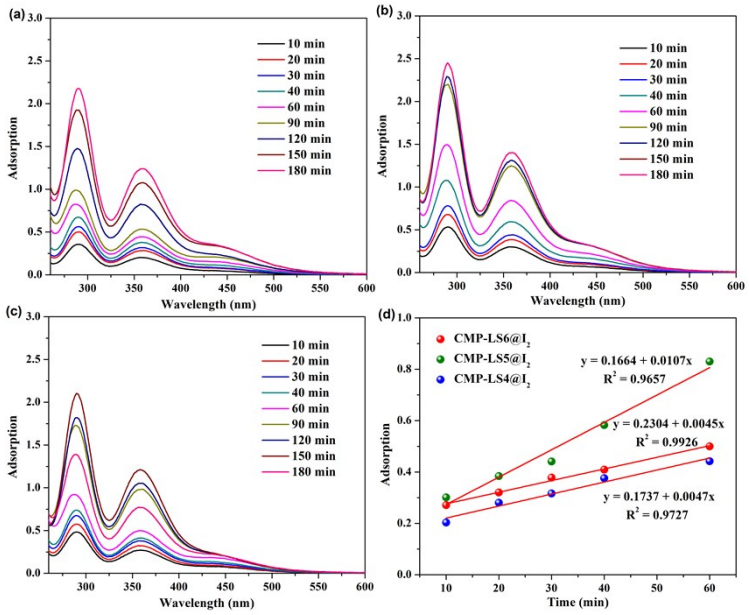

Fig. S15 UV-vis spectra of iodine released from **I_2@CMP-LS4** (a), **I_2@CMP-LS5** (b), **I_2@CMP-LS6** (c) (2 mg in 10 mL of ethanol); (b) the release rate of **I_2@CMP-LS4–6** in ethanol.

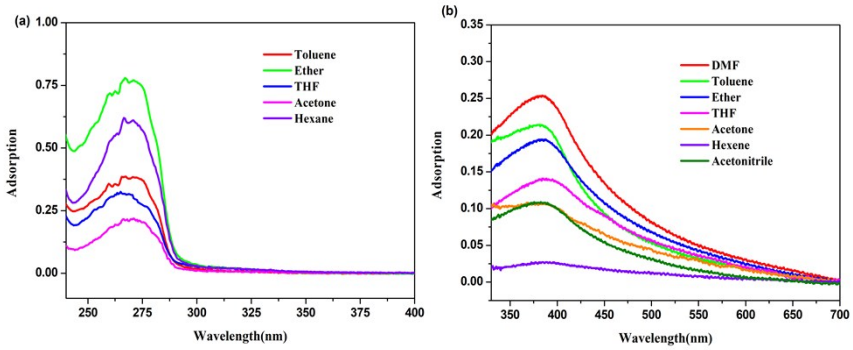

Fig. S16 UV-vis spectra of **CMP-LS4** (a) and **CMP-LS5** (b) in various solvents.

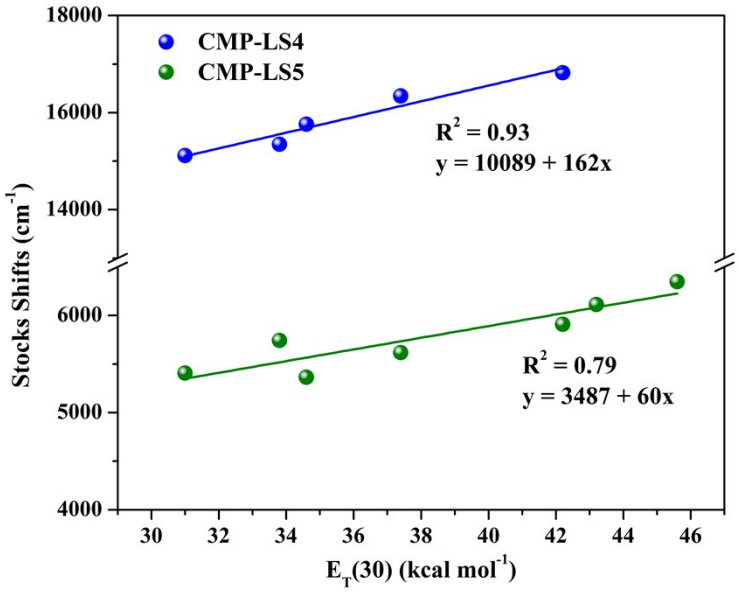

Fig. S17 Plots of Stokes shifts of **CMP-LS4** and **CMP-LS5** versus the solvent polarity parameter $E_T(30)$.

Table S1 Summary of CO_2 adsorption amount and heat of adsorption in porous organic polymers.

POPs	CO_2 uptake mmol/g	Q_{st} kJ/mol	Ref.
CMP-LS4	1.29	38.1	our work
CMP-LS5	2.68	34.7	
CMP-LS6	1.56	33.3	
PAF-1	2.05	15.6	*Energy Environ. Sci* ., 2011, **4**, 3991–3999.
PAF-3	3.48	19.2	
PAF-4	2.41	16.2	
CMP-1-COOH	2.05	33	*Chem. Sci.* , 2011, **2**, 1173–1174.
CMPN-1	0.98	28.2	*J. Mater. Chem. A*, 2015, **3**, 87–91.
CMPN-2	1.67	30.2	
CMPN-3	0.87	26.5	
N-rich polymer	2.22	33.7	*Polym. Chem.* , 2018, **9**, 2643–2649.
PAN-2	1.97	39.3	*Macromolecules* , 2014, **47**, 6664−6670.
POPs-B10	3.2	17.35	*Polym. Chem.* , 2017, **8**, 1833–1839.
POPs-B20	3.29	13.87	
BTLP-4	4.31	28.7	*J. Mater. Chem. A*, 2017, **5**, 258–265.
BTLP-5	3.15	29.1	
NO2-PAF-1	1.14	38.4	*Polym. Chem.* , 2016, **7**, 770–774.
CTF-BIB-1	4.33	35.2	*ACS Appl. Mater. Interfaces* , 2018, **10**, 26678–26686.
CTF-BIB-2	4.12	34.7	
CTF-BIB-3	3.86	32.5	
PAF-1	2.05	15.6	*Energy Environ. Sci.* , 2012, **5**, 8370–8376.

Table S2 Summary of surface area and iodine sorption properties of POPs and other porous adsorbents.

Sample	BET (m^2 g^{-1})	Iodine uptake (g g^{-1})	T (□)	Ref.
CMP-LS4	462	3.32	80	*This work*
CMP-LS5	1158	4.4		
CMP-LS6	679	2.44		
SCMP-1	413	1.88	80	*ACS Appl. Mater. Interfaces* , 2016, **8**, 21063–21069.
SCMP-2	855	2.22		
SCMP-□	119.76	3.45	80	*Chem. Commun.* , 2016, **52**, 9797–9800.
Azo-Trip	510.4	2.33	77	*Polym. Chem.* , 2016, **7**, 643–647.
NTP	1067	1.8	75	*ACS Macro Lett.* , 2016, **5**, 1039–1043.
PAF-23	82	2.71	75	*Angew. Chem. Int. Ed.* , 2015, **54**, 12733–12737.
PAF-24	136	2.76		
PAF-25	262	2.6		
BDP-CPP-1	635	2.83	75	*J. Mater. Chem. A* , 2017, **5**, 6622–6629.
BDP-CPP-2	235	2.23		
NBDP-CPP	658	1.5		
TTPA	315.5	1.77	77	*Polym. Chem.* , 2018, **9**, 777–784.
TTPB	222.25	4.43	77	*J. Mater. Chem. A* , 2017, **5**, 9612–9617.
TTPPA	512.39	4.9	77	*J. Mater. Chem. A* , 2018, **6**, 2808–2816.
TTDAB	1.643	3.13		
Tm-MTDAB	2.778	3.04		
PAF-1	5600	1.86	25	*J. Mater. Chem. A* , 2014, **2**, 7179–7187.
JUC-Z2	2081	1.44		
ZIF-8	1875	1.2	75	*Ind. Eng. Chem. Res.,* 2012, **51**, 614–620.
HKUST-1	1798	1.5		
Cu-BTC	1500-1800	1.75	75	*Chem. Mater.,* 2013, **25**, 2591–2596.

Table S3 Summary of pore volume of **CMP-LS4–6**.

Sample	V_{total}/cm^3 g^{-1}	V_{micro}/cm^3 g^{-1}	V_{extra}/cm^3 g^{-1}
CMP-LS4	0.31	0.13	0.18
CMP-LS5	1.36	0.28	1.08
CMP-LS6	1.26	0.07	1.19